

Structure, superfluidity, and quantum melting of hydrogen clusters

Fabio Mezzacapo¹ and Massimo Boninsegni^{1,2}

¹*Department of Physics, University of Alberta, Edmonton, Alberta, Canada T6G 2J1*

²*INFN-BEC, Dipartimento di Fisica, Universita' degli Studi di Trento, Via Sommarive 4, I-38050 Povo, Italy*

(Received 5 December 2006; published 14 March 2007)

We present results of a theoretical study of para-H₂ (*p*-H₂) and ortho-D₂ (*o*-D₂) clusters at low temperature (0.5 K ≤ *T* ≤ 3.5 K) based on path integral Monte Carlo simulations. Clusters of *N* ≤ 21 *p*-H₂ molecules are nearly entirely superfluid at *T* ≤ 1 K. For 22 ≤ *N* ≤ 30, the superfluid response displays strong variations with *N*, reflecting structural changes that occur on adding or removing even a single molecule. Some clusters in this size range display *quantum melting*, going from solidlike to liquidlike as *T* → 0. Melting is caused by quantum exchanges of molecules. The largest *p*-H₂ cluster for which a significant superfluid response is observed comprises *N* = 27 molecules. Evidence of a finite superfluid response is presented for *o*-D₂ clusters of size up to *N* = 14. Magic numbers are observed, at which both types of clusters feature pronounced stability.

DOI: [10.1103/PhysRevA.75.033201](https://doi.org/10.1103/PhysRevA.75.033201)

PACS number(s): 36.40.-c, 67.90.+z, 61.25.Em

I. INTRODUCTION

The search for superfluidity (SF) in condensed phases of atomic or molecular species other than helium is the subject of a significant investigative effort, from both theoretical and experimental standpoints. Fluids made of light bosonic molecules such as para-hydrogen (*p*-H₂) or ortho-deuterium (*o*-D₂), whose mass is smaller than (or equal to) that of helium atoms, have long been regarded as potential superfluids [1]. However, the attractive interaction between two hydrogen molecules results in an equilibrium crystal phase, with a freezing temperature higher than that at which a superfluid transition might take place [2].

Confinement and reduction of dimensionality are deemed plausible avenues to stabilize a metastable liquid phase down to temperatures sufficiently low that a superfluid transition may be observed. However, theoretical studies of *p*-H₂ films adsorbed on various substrates [3–5], as well as in two mathematical dimensions [6], have so far yielded no hint of possible SF. The suggestion was made that SF may occur in a strictly two-dimensional (2D) *p*-H₂ fluid embedded in a crystalline matrix of alkali-metal atoms [7]. That prediction was actually based on numerical simulations of model systems of very small size, and there is evidence that the observed superfluid signal is merely a finite-size effect [8].

On the other hand, sufficiently small clusters can remain “liquidlike” at significantly lower *T* than the bulk, and therefore SF could occur at temperatures that may render its observation possible [9]. For example, a recently introduced experimental technique, known as helium nanodroplet isolation spectroscopy (HENDI), allows one to investigate a single molecular impurity embedded in clusters comprised from a few to several thousand He atoms [10]. In these experiments, SF of the medium surrounding the molecule (i.e., the cluster) can be inferred by studying the rotational spectrum of the dopant. Specifically, the observed decoupling of the rotation of the molecule from that of the cluster signals the onset of SF in the cluster. Evidence of SF has been found at *T* < 1 K in helium clusters surrounding a linear carbonyl sulfide (OCS) impurity and, with the same technique, in clusters of *N* = 14–16 *p*-H₂ molecules surrounding the same im-

purity; these clusters are enclosed in a larger helium droplet [11,12]. The same experiment failed to detect superfluid behavior of *o*-D₂ clusters.

These observations constitute the starting point for an intense theoretical effort, aimed at gaining a deeper understanding of SF in clusters of *p*-H₂ and, possibly, *o*-D₂ molecules. Quantum Monte Carlo (QMC) methods appear to be the most powerful theoretical tool to attack such an interesting problem and have already been successfully employed to characterize the structure and SF of doped ⁴He clusters both at finite and zero temperature [13–16]. For instance, path integral Monte Carlo (PIMC) simulations have yielded evidence of SF in (*p*-H₂)_{*N*} clusters seeded with an OCS molecule [OCS@(*p*-H₂)_{*N*}], for 10 ≤ *N* ≤ 17, as well as in smaller complexes such as OCS@(*p*-H₂)₅ and OCS@(*o*-D₂)₅ [17–19]. Reptation Quantum Monte Carlo simulations have provided information about the structure of CO@(*p*-H₂)_{*N*}, for *N* ~ 12, and have clarified some features of the experimentally measured infrared spectra [20,21].

Obviously, of crucial importance to the full characterization of the experiments, as well as to the understanding of the microscopic origin of SF, remains the study of pristine (i.e., undoped) clusters. In this sense, hydrogen is even richer a playground than helium. For example, *p*-H₂ and *o*-D₂ clusters provide a unique opportunity to study the effect of mass on the superfluid and structural properties of such a small systems, because the *o*-D₂ molecular mass is twice that of *p*-H₂, while the intermolecular interaction is very nearly the same. Moreover, because the equilibrium phase of hydrogen is crystalline at low *T*, studying clusters of molecular hydrogen offers insight in the evolution of the physical properties as the number of particles is increased.

The first theoretical investigation of pure *p*-H₂ clusters, based on PIMC simulations, was published in 1991; it was restricted to three cluster sizes: namely, *N* = 13, 18, and 33. Two clusters were found to be superfluid and “liquidlike,” while (*p*-H₂)₃₃ was observed to be “solidlike” at *T* ≤ 2 K [22].

In a recent article, we carried out a systematic study of the physical properties of *p*-H₂ clusters as a function of both size and temperature (*N* ≤ 40 and 0.5 K ≤ *T* ≤ 4 K) [23]. Such a

study was based on PIMC simulations making use of a recently introduced *worm* algorithm (WA)[24]. Specifically, we computed superfluid fraction ρ_S and density profiles, pointing out the remarkable dependence on N of ρ_S , for $22 \leq N \leq 30$, and how, in this size range, some clusters display coexistence of insulating (solidlike) and superfluid (liquidlike) phases, with the latter, induced by zero-point motion and quantum exchanges, becoming dominant as T is lowered. We refer to this peculiar behavior as “quantum melting.” Although experimental data for pristine clusters are not yet available, novel techniques based on Raman spectroscopy may soon be able to isolate pure clusters and characterize their superfluid properties [25].

The purpose of the present paper is twofold; on the one hand, we provide additional results for p -H₂ clusters, chiefly the energetics but also for the superfluid fraction [$\rho_S(T)$] and the structure of the clusters as a function of their size, and also compare results obtained with different intermolecular potentials. We also offer an expanded discussion of the material presented in Ref. [23]. Moreover, we present novel results for pure o -D₂ clusters of size up to $N=20$ molecules, down to $T=0.5$ K. We report superfluid behavior of o -D₂ clusters of as many as 14 molecules; in these clusters as well, structure and superfluid response are closely related and non-trivially dependent on N . Specific clusters [i.e., (o -D₂)₁₃ and (o -D₂)₁₉] feature greater stability, confirming the existence of “magic” numbers N of molecules.

The remainder of this paper is organized as follows: in the next section, we describe our microscopic model Hamiltonian and offer basic details of our simulations (the reader is referred to Ref. [24] for a full description of the WA). In Sec. III we present and discuss our findings. In particular, we provide additional details on our results previously published in Ref. [23] and illustrate our new numerical data for both p -H₂ and o -D₂ pure clusters. Finally, we outline the main physical conclusions of our work.

II. METHODOLOGY

We model the system of our interest as a collection of N p -H₂ (o -D₂) molecules, regarded as point particles. The quantum mechanical Hamiltonian is the following:

$$H = -\lambda \sum_i^N \nabla_i^2 + V(\mathbf{R}), \quad (1)$$

where $\lambda = 12.031 \text{ K } \text{\AA}^2$ for p -H₂ (half this value for o -D₂), $\mathbf{R} \equiv \mathbf{r}_1, \mathbf{r}_2, \dots, \mathbf{r}_N$ is a collective coordinate referring to all N particles in the system, and $V(\mathbf{R})$ is the total potential energy of the configuration \mathbf{R} .

In most of the published numerical work on clusters of molecular hydrogen, the potential energy V is expressed as a sum of pairwise contributions, each represented by a spherically symmetric potential; this work is no exception in this regard. For the majority of our calculations, we have made use of the Silvera-Goldman (SG) pair potential [26], which is the most commonly employed in previous investigations. For comparison purposes, however, we have also obtained results with a different intermolecular potential, due to Buck and co-workers [27–29].

Our simulations are carried out by means of a *canonical* variant of the WA presented in Refs. [24]. The only difference, with respect to the fully *grand canonical* implementation, is that all the so-called Z-sector configurations (which are utilized to compute thermodynamic expectation values) have the same number of particles (i.e., there are no fluctuations of N); this proves more convenient than a fully grand canonical implementation, as we are interested in characterizing properties of clusters as a function of N . As in any PIMC simulation, a high-temperature approximation for the many-body density matrix is required, and we have used one that is accurate up to fourth order [30] in the imaginary time step ϵ ; we empirically found the value $\epsilon = 1/640 \text{ K}^{-1}$ to yield estimates indistinguishable, within our quoted statistical uncertainties, from those extrapolated to the $\epsilon \rightarrow 0$ limit (i.e., the limit where the method becomes formally *exact*). We used in our calculations a cubic box of 50 \AA side, with periodic boundary conditions (PBC’s) [31]. In previous calculations (e.g., Ref. [22]), an artificial confining potential was adopted, in order to prevent molecules from evaporating (i.e., to keep the clusters together). We found this device unnecessary, as all the clusters studied here stay together, with no sign of evaporation, without such an external potential.

As mentioned above, in the present work we computed energetics, radial density profiles, and the superfluid fraction $\rho_S(T)$ of p -H₂ and o -D₂ clusters. All of the estimates reported here, as well as the physical effects discussed in the next section, are observed to be independent of the initial configuration of the clusters.

In a finite system and within the PIMC formalism, it can be shown [32] that $\rho_S(T)$, defined as the fraction of the system that decouples from an externally induced rotation, is expressed by

$$\rho_S(T) = \frac{4m^2T}{\hbar^2 I_c} \langle A^2 \rangle. \quad (2)$$

Here, $\langle \dots \rangle$ stands for thermal average, I_c is the classical moment of inertia of the cluster, and A is the total area swept by the many-particle paths, projected onto a plane perpendicular to one of the three equivalent rotation axes.

III. RESULTS

In this section we present our results for pure p -H₂ and o -D₂ clusters. Some of the results shown for the superfluid density of p -H₂ clusters have appeared in Ref. [23]. The results for o -D₂ clusters are presented in the last subsection, in which we also point out differences and similarities between p -H₂ and o -D₂ clusters.

A. p -H₂ clusters

1. Energetics

The total energy per p -H₂ molecule $e(N)$ as a function of the cluster size N , at $T=1$ K, computed using the SG potential, is shown in Fig. 1. Also shown in the figure are the estimates from Ref. [22]. For comparison purposes, we also

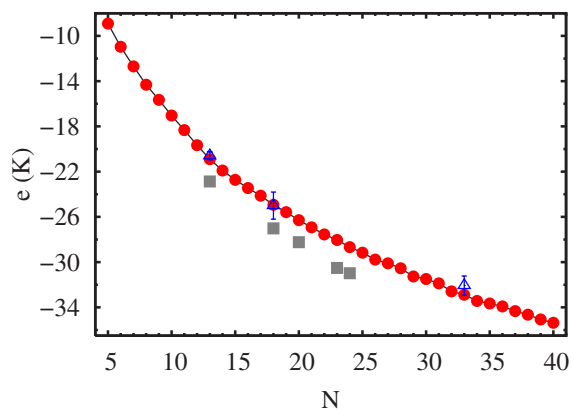


FIG. 1. (Color online) Energy per p -H₂ molecule versus cluster size N , at $T=1$ K. Estimates have been obtained using the SG (circles) and Buck (boxes) potentials. When not shown, statistical errors are of the order of, or smaller than, the symbol size. The solid line is only a guide to the eye. Also shown for comparison are results from Ref. [22] (triangles).

furnish energetics based on the Buck potential; in this case, binding energies are considerably greater than those computed with the SG interaction. For example, a cluster of 23 molecules is characterized by an energy some 2.5 K more negative than that obtained with the SG potential. Such a difference can be simply ascribed to the deeper attractive well (roughly 2 K at the minimum) of the Buck potential.

The energy values shown in Fig. 1 for the Buck potential are generally consistent with those reported in a recent paper by Guardiola and Navarro [34], who computed them at $T=0$ by means of diffusion Monte Carlo simulations [35]. However, for some clusters our energies are significantly lower than those of Ref. [34]. For example, for $N=23$ the value quoted in Ref. [34] is $-29.94(2)$ K, whereas our own value at $T=1$ K is $-30.513(15)$ K. At present, the reason for such a discrepancy is unknown. We note, however, that our data for the Buck potential are in agreement with those obtained independently by other authors, using $T=0$ QMC methods [36,37].

The energy per p -H₂ molecule is a monotonically decreasing function of the cluster size; the simple formula

$$e(N) = A_V + A_S N^{-1/3} + A_C N^{-2/3}, \quad (3)$$

where A_V , A_S , and A_C are the well-known volume, surface, and curvature terms, fails to yield a reasonable fit to our data, as well as an accurate extrapolation of the bulk energy (~ -90 K), to indicate that the physics of the bulk is not yet approached by clusters of size studied here. This should be compared with the case of small ⁴He clusters (of size up to $N=50$), for which the same formula provides an acceptable fit to the data, even though the extrapolated bulk energy differs from the actual value by over 0.5 K [33].

Because in the case of helium the equilibrium condensed phase is liquid, no qualitative structural change occurs as the size of the cluster is increased. For hydrogen, on the other hand, the structure must evolve from liquidlike to solidlike, presumably in a nonmonotonic fashion, but rather going through structures of different shapes and geometries. It is

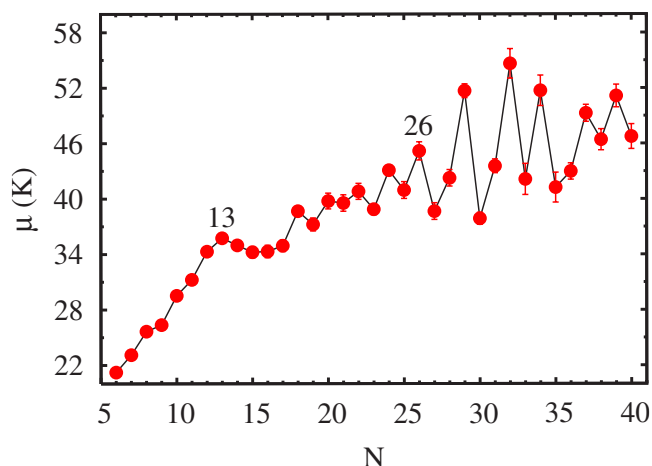


FIG. 2. (Color online) Chemical potential of p -H₂ clusters versus cluster size N . When not shown, statistical errors are of the order of, or smaller than, the symbol size. The solid line is only a guide to the eye. Numbers refer to stable (“magic”) clusters.

therefore scarcely surprising that a simple formula like Eq. (3) should not offer equally acceptable a fit as for helium clusters.

Recent $T=0$ QMC calculations [34,36] have pointed out the existence of magic sizes (i.e., $N=13$) corresponding to particularly stable clusters. In order to have a clear visual identification of these magic sizes, we plot in Fig. 2 the chemical potential μ as a function of the cluster size defined as [35]

$$\mu(N) = E(N-1) - E(N), \quad (4)$$

where $E(N)$ is the total energy of a cluster of N molecules.

The chemical potential increases monotonically for $N \leq 13$; for clusters of greater size, its behavior is rather irregular. Local maxima are observed for particular values of N (i.e., $N=13$ and 26). The corresponding clusters are characterized by considerable stability and rather compact structure.

In the following, we show that p -H₂ clusters of size $N < 22$ display properties consistent with a liquidlike superfluid character; the stability of $(p\text{-H}_2)_{13}$ is, in our view, not the sign of the occurrence of a particular solidlike structure, as proposed in Ref. [34], but rather of first shell completion (which does not rule out liquidlike behavior) [25,20]. On the other hand, as clarified below, the peak of the chemical potential observed at $N=26$ reflects the distinct solidlike behavior of the cluster $(p\text{-H}_2)_{26}$.

2. Superfluidity

Data for the superfluid fraction $\rho_S(T)$ of $(p\text{-H}_2)_{18}$ are shown in Fig. 3. As expected, $\rho_S(T)$ is a monotonic decreasing function of T ; this cluster is essentially entirely superfluid (i.e., $\rho_S(T) \approx 1$) at $T \leq 1$ K. Then, $\rho_S(T)$ drops to a value ~ 0.27 in a temperature interval of 1.5 K and decreases more slowly at higher T .

A finite system cannot undergo a phase transition in a strict sense; therefore, in order to assign a “transition tem-

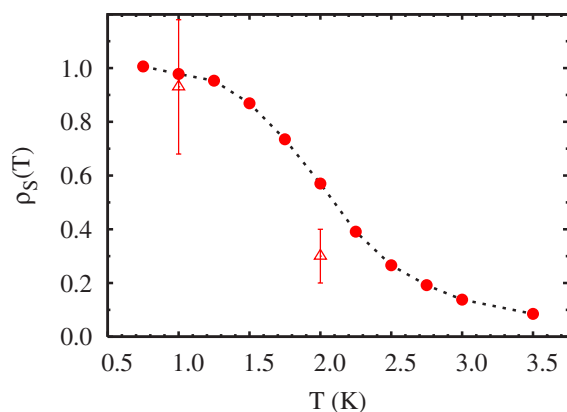


FIG. 3. (Color online) Temperature dependence of the superfluid fraction $\rho_S(T)$ for a clusters of 18 p -H₂ molecules (circles). The dotted line is only a guide to the eye. When not shown, statistical errors are smaller than the symbol size. Also shown for comparison are results from Ref. [22] (triangles).

perature,” one must resort to some arbitrary criterion. Because the notion of superfluid fraction is scarcely meaningful when the average number of molecules in the superfluid phase is ~ 1 , we empirically define our “transition temperature” T_c as that at which $N\rho_S(T_c) \approx 2$. Hence the estimated transition temperature is $T_c \approx 3$ K.

The superfluid fraction computed with the SG potential (circles) as a function of the cluster size at $T=1$ K is presented in Fig. 4 [38]. Clusters of size $N < 22$ are entirely superfluid (or nearly so, at least within the precision of our calculations) and display a temperature dependence of the superfluid fraction similar to that shown in Fig. 3 for $N=18$.

An interesting, nonmonotonic trend is observed (Fig. 4) for the superfluid fraction at low T of clusters of $22 \leq N \leq 30$ molecules. The value of $\rho_S(T=1$ K) is close to unity for $N=22$ and drops to a local minimum if a single molecule is added (i.e., for $N=23$). It then rises again to approximately 85%, if another molecule is added ($N=24$), and remains rela-

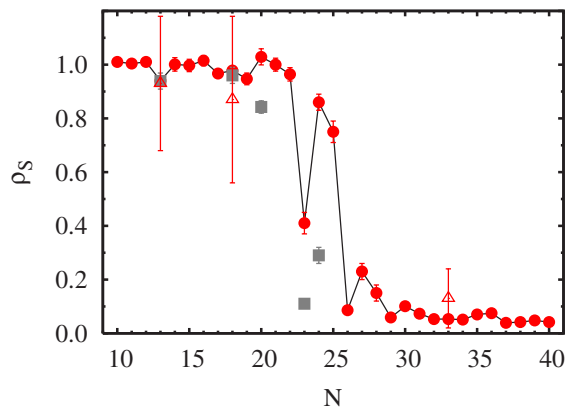


FIG. 4. (Color online) Superfluid fraction of p -H₂ clusters versus cluster size N , at $T=1$ K. Estimates have been obtained using the SG (circles) and Buck (boxes) potentials. When not shown, statistical errors are of the order of, or smaller than, the symbol size. The solid line is only a guide to the eye. Also shown for comparison are results from Ref. [22] (triangles).

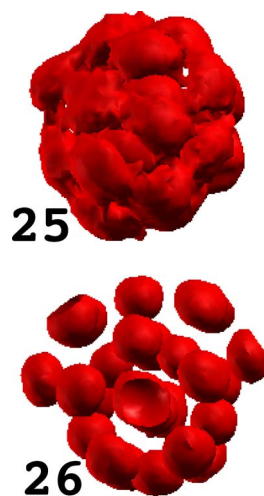


FIG. 5. (Color online) Three-dimensional representation of a cluster comprising 25 and 26 p -H₂ molecules at a temperature of 1 K. Even though the information provided by this kind of figure is purely qualitative, the structural difference is evident: $(p\text{-H}_2)_{25}$ is essentially liquidlike (molecules are highly delocalized), while $(p\text{-H}_2)_{26}$ is solidlike (molecules are more localized and clearly distinguishable).

tively large for $N=25$. The addition of another molecule, from $N=25$ to $N=26$, again causes an abrupt drop of ρ_S , to less than 0.1. On adding one more molecule, ρ_S becomes again significant (approximately 25%), but drops sharply once more at $N=29$; it remains small, while still featuring noticeable oscillations, for greater N values.

Generally speaking, as the number N of particles increases, the physics of a cluster ought to approach that of the bulk; in its bulk phase at low T , p -H₂ is an insulating (non-superfluid) crystal—i.e., its character is completely different from that of small clusters (i.e., $N < 22$), which remain liquidlike and are entirely superfluid. The data in Fig. 4 show how the evolution from liquidlike to solidlike does not occur continuously; i.e., bulk properties do not gradually emerge when N increases.

In particular, we interpret the peculiar behavior of ρ_S observed for $22 \leq N \leq 30$ as due to alternating superfluid (liquidlike) or insulating (solidlike) character of the clusters. It seems plausible that drastic changes of the superfluid fraction, occurring upon adding just one molecule, ought to be directly connected with structural changes.

In order to illustrate this point, we show in Fig. 5 graphical representations of the three-dimensional structure of a p -H₂ cluster consisting of 25 and 26 molecules at $T=1$ K; these figures are produced as explained in Ref. [20]. The cluster $(p\text{-H}_2)_{26}$ displays remarkably solidlike properties. Its structure consists of three rings of five molecules, with four other molecules linearly arranged along the axes of the rings, while the remaining seven molecules form an outer shell. Although their position is smeared by zero-point fluctuations, the various molecules in the cluster can be clearly identified, indicating that they enjoy a fairly high degree of spatial localization; consequently, exchanges among different molecules are highly suppressed (though not completely absent, as shown in Fig. 6) and the superfluid response is weak.

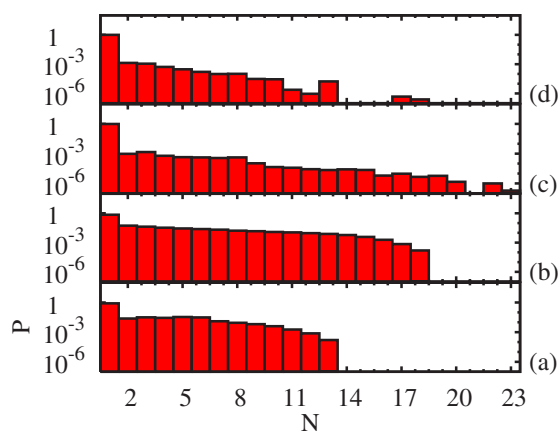


FIG. 6. (Color online) Statistics of permutation cycles involving N molecules for the clusters $(p\text{-H}_2)_{13}$ (a), $(p\text{-H}_2)_{18}$ (b), $(p\text{-H}_2)_{26}$ (c), and $(p\text{-H}_2)_{33}$ (d) at $T=1$ K.

Conversely, the molecules in the cluster $(p\text{-H}_2)_{25}$ cannot be clearly identified and the entire system appears amorphous. Because of their pronounced delocalization, molecules have a strong propensity to be involved in quantum exchanges, hence the large superfluid response observed. The physics is reminiscent of that of the insulating-superfluid quantum phase transition observed in lattice models of hard core bosons, where a superfluid, noncrystalline phase appears as the system is driven away from commensuration (where it is an insulator) [40].

Figure 6 shows the statistics of exchange cycles involving N molecules for the clusters (from bottom to top) $(p\text{-H}_2)_{13}$, $(p\text{-H}_2)_{18}$, $(p\text{-H}_2)_{26}$, and $(p\text{-H}_2)_{33}$ at a temperature $T=1$ K. Long exchange cycles are known to underlie superfluidity. The value of the superfluid fraction of the smaller clusters (i.e., $N=13$ and 18) is close to 1, and exchanges occur involving up to N molecules, with significant frequency. On the other hand, in the case of $(p\text{-H}_2)_{26}$ and $(p\text{-H}_2)_{33}$, ρ_S is less than 0.1; remarkably, however, exchange cycles involving as many as 23 and 18 molecules, respectively, have finite, albeit small, statistical weight. This observation is consistent with that made in Ref. [39] (based on a PIMC simulation which did not explicitly include exchanges).

The superfluid fraction computed with the Buck potential (boxes in Fig. 4) is in excellent agreement with that obtained with the SG for those clusters that are liquidlike (i.e., with $N \leq 22$). Quantitative differences (i.e., lower values of ρ_S obtained with the Buck potential, as shown in Fig. 4) occur for larger clusters (which generally display more solidlike behavior), due to the more attractive character of the Buck potential, which results in greater molecular localization. However, the observed trend is qualitatively identical.

3. Quantum melting

Some clusters in the size range $22 \leq N \leq 30$ feature a fascinating behavior in the temperature range explored in this work; we discuss in detail the case of $(p\text{-H}_2)_{23}$, for which the superfluid fraction takes a local minimum. Figure 7 shows the values of the superfluid fraction and of the potential energy per molecule, recorded during a typical Monte Carlo

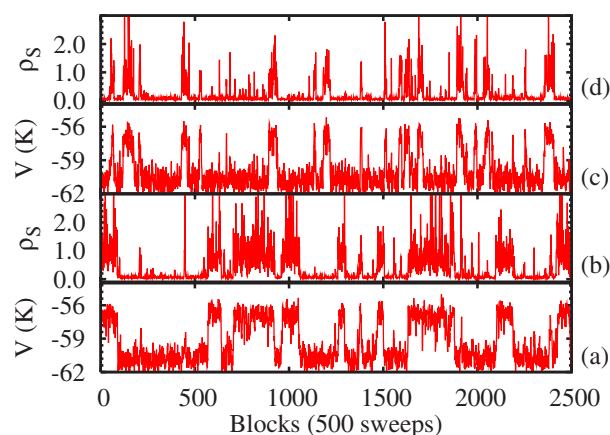


FIG. 7. (Color online) Potential energy per molecule and superfluid fraction observed during a typical Monte Carlo run (see text) for a cluster of $N=23$ $p\text{-H}_2$ molecules at $T=1$ K [panels (a) and (b)] and $T=1.4$ K [panels (c) and (d)]. The coexistence of two phases can be easily recognized since the averages of ρ_S and V simultaneously switch between high (liquidlike superfluid phase) and low (solidlike insulating phase) values. The liquidlike superfluid phase becomes dominant as T is lowered.

run for a cluster of 23 $p\text{-H}_2$ molecules at $T=1.4$ K and $T=1$ K. In particular, we show consecutive block averages of ρ_S and V , each block consisting of 500 sweeps [41].

Despite the large fluctuations affecting the values of ρ_S , two different regimes can be easily identified: one in which the superfluid fraction is high, with an average value close to 1, and the other characterized by low values of ρ_S , with an average value close to zero. The potential energy, correspondingly, takes on high (low) values when ρ_S is large (small). While the behavior of the superfluid fraction is consistent with the coexistence of two phases, characterized by large and small superfluid response, the information given by the potential energy suggests that these two phases have also liquidlike and solidlike properties. The switching of the average value of the potential energy between two different regimes, separated by some ~ 6 K, can be interpreted as due to the system visiting relatively ordered, solidlike, insulating configurations (characterized by low potential energy) and disordered, liquidlike, superfluid ones. The coexistence between two distinct (disordered and ordered) phases is consistent with the observation made in Ref. [42] for classical clusters.

On decreasing the temperature from $T=1.4$ K [panels (c) and (d) of Fig. 7] to $T=1$ K [panels (a) and (b) of the same figure], the superfluid (liquidlike) phase (i.e., large values of ρ_S and V) is observed during a greater fraction of the simulation time and becomes dominant as T approaches 0 K; the cluster therefore “melts” at low T . This process is ostensibly induced by zero-point motion and the ensuing exchanges of molecules, whose importance increases as T is lowered. In this sense, one could state that melting is driven by Bose statistics; i.e., it is associated with the energy contribution due to quantum exchanges.

On the other hand, when T is sufficiently high, quantum exchanges are suppressed and the system “freezes” in a solidlike structure. Evidence of such *quantum melting* has also

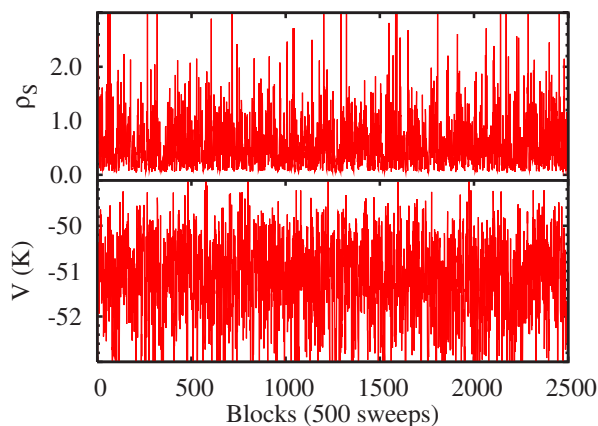


FIG. 8. (Color online) Potential energy per molecule and superfluid fraction recorded during a typical Monte Carlo run for a cluster of $N=18$ p -H₂ molecules at $T=2$ K. In this case, ρ_S and V simply oscillate around their average values (approximately 0.6 for ρ_S) without featuring the clear, simultaneous “jumps” observed in Fig. 7. This system is found to be liquidlike in the range of temperature considered in this work.

been found for $(p\text{-H}_2)_{27}$. Other clusters in the size range $22 \leq N \leq 30$ presumably display the same physics, albeit at lower T . It is important to stress that the behavior illustrated in Fig. 7 is different than that of a cluster that is liquidlike and simply not 100% superfluid; indeed, in such a case the superfluid fraction and potential energy merely fluctuate around their average values, with no evidence of the switching displayed in Fig. 7. This is precisely what we find for clusters of size $N < 22$, which are liquidlike at all temperatures, with superfluid (normal) component growing at low (high) T (see Fig. 8).

Our interpretation is supported by the evolution with T of the radial density profiles $\rho(r)$ of the cluster, defined with respect to its center of mass. In Fig. 9, radial density profiles for $(p\text{-H}_2)_{23}$ and $(p\text{-H}_2)_{18}$ at $T=0.75$ K (diamonds and boxes) as well as at $T=2$ K (stars and triangles) are shown. A

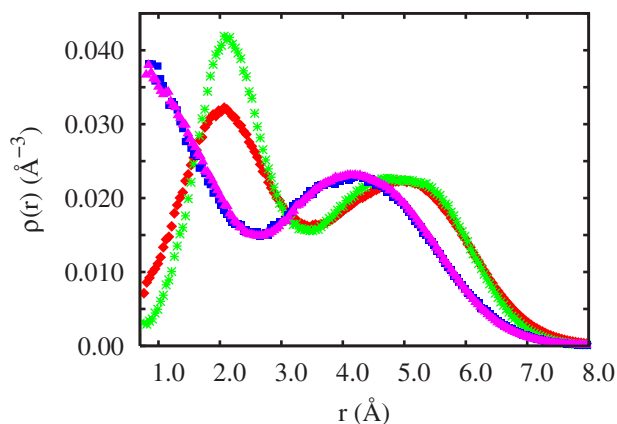


FIG. 9. (Color online) Radial density profiles for a p -H₂ cluster with $N=18$ [$T=0.75$ K (boxes) and $T=2$ K (triangles)] and $N=23$ [$T=0.75$ K (diamonds) and $T=2$ K (stars)] p -H₂ molecules. Statistical errors, not shown for clarity, are of the order of $5 \times 10^{-4} \text{ \AA}^{-3}$ or less.

cluster comprising 23 p -H₂ molecules at a temperature $T=2$ K displays a two-shell structure with one sharp peak at $r \approx 2 \text{ \AA}$ and a second broader one at about 5.5 \AA . As T is lowered to 0.75 K, the first peak becomes significantly broader and its height decreases. Therefore, molecules in the inner shell are less localized and the cluster is more liquidlike, with greater propensity for quantum exchanges both in the first shell and between the first and second shells. For a cluster of 18 molecules, on the other hand, density profiles stay the same, as T is lowered from 2 K to 0.75 K, featuring one particle in the center of mass [signaled by the large value of $\rho(r \rightarrow 0)$] and an outer shell, separated by a shallow minimum (indicative of liquidlike structure). The value of the superfluid fraction of $(p\text{-H}_2)_{18}$ increases from about 0.57 to roughly 1 when T goes from 2 K to 0.75 K; however, this change is hardly reflected in the cluster structure. Quite differently, the increase of ρ_S in a cluster of 23 molecules, observed in the same temperature range, reflects a substantial change in the structure, due to quantum melting (as shown in Fig. 9). This phenomenon clearly exemplifies the importance of quantum effects on the structural properties of small systems, which has been also investigated in clusters of neon, which display moderate quantum character [43–46].

We conclude by stressing once again that, even though the results presented in this section are obtained using the SG potential, similar physics is observed if the more attractive Buck potential is adopted. The only quantitative changes are the values of the superfluid fraction, which are generally lower than those computed with the SG interaction for a given T . However, quantum melting is observed in clusters of the same size, even if the potential due to Buck and co-workers is used; i.e., it is broadly independent of the details of the interaction.

B. o -D₂ clusters

Next, we discuss the properties of o -D₂ clusters; here, too, we regard o -D₂ molecules as bosons of spin zero [47], with a mass twice that of p -H₂ molecules. We computed the energy, superfluid fraction, and radial density profiles for clusters of size N ranging from 3 to 20 molecules at $0.5 \text{ K} \leq T \leq 2.0 \text{ K}$.

1. Energetics

The total energy per o -D₂ molecule as a function of the cluster size at $T=0.5$ K is shown in Fig. 10. For $N=3$, the energy has a value close to -9 K, which smoothly decreases with N , reaching a value of roughly -36 K for $N=12$. On adding one more molecule, the energy drops to about -39.5 K ($N=13$) and decreases more slowly for N up to 17. For greater values of N an important drop of the energy is still observed at $N=19$. As in the previously discussed case of p -H₂ clusters, a fit of our data using Eq. (3) is difficult and does not allow an accurate estimate of the bulk energy; moreover, the chemical potential (see Fig. 11) displaying sharp local maxima for $N=13$ and 19 confirms the existence of “magic” sizes, corresponding to highly stable clusters [i.e., $(o\text{-D}_2)_{13}$ and $(o\text{-D}_2)_{19}$].

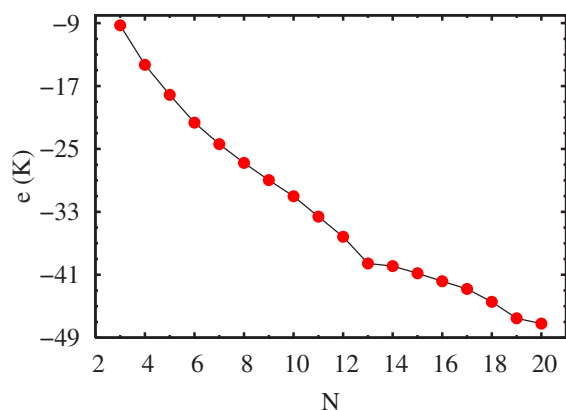


FIG. 10. (Color online) Energy per o -D₂ molecules e versus cluster size N at a temperature of 0.5 K. Statistical errors are smaller than the symbol size. The solid line is only a guide to the eye.

2. Superfluidity

Figure 12 shows $\rho_S(T)$ for a cluster of 11 o -D₂ molecules. The monotonically decreasing trend is qualitatively similar to that in Fig. 3 for $(p$ -H₂)₁₈. However, the superfluid fraction of the cluster $(o$ -D₂)₁₁ decreases more rapidly with T . In particular, it is approximately 1 at $T \leq 0.5$ K and suddenly drops to a value ≈ 0.39 (corresponding to roughly 4 molecules in the superfluid phase) when T increases of 0.5 K. At higher temperature, the superfluid fraction becomes essentially zero (in the sense explained in the previous section) for $T \approx 1.4$ K, at which the average number of molecules in the superfluid phase is less than 2. It is important to note that, while the cluster $(p$ -H₂)₁₈ is almost 60% superfluid at $T=2$ K (Fig. 3), $(o$ -D₂)₁₁ at the same temperature is non-superfluid and the probability of observing permutation cycles comprising more than 3 o -D₂ molecules is less than 5×10^{-4} . The statistics of many-particle permutations in the system $(o$ -D₂)₁₁ at $T=0.5$ K (lower panel) and 2 K (upper panel) shown in Fig. 13 points out how, at high T , long exchange cycles disappear, as clusters behave more classically.

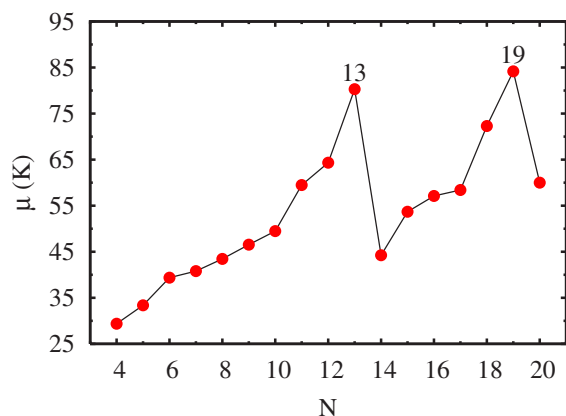


FIG. 11. (Color online) Chemical potential of o -D₂ clusters versus cluster size N . When not shown, statistical errors are of the order of, or smaller than, the symbol size. The solid line is only a guide to the eye. Numbers refer to stable (“magic”) clusters.

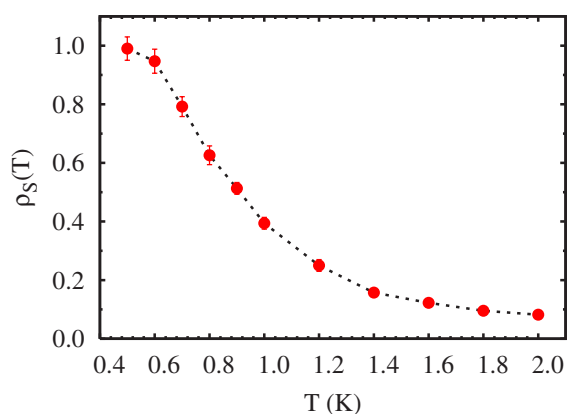


FIG. 12. (Color online) Temperature dependence of the superfluid fraction $\rho_S(T)$ for a clusters of 11 o -D₂ molecules. The dotted line is only a guide to the eye. When not shown, statistical errors are smaller than the symbol size.

The size dependence of the superfluid fraction at two different temperatures ($T=0.5$ and 2 K) is shown in Fig. 14. At $T=0.5$ K, small o -D₂ clusters ($N \leq 9$) are entirely superfluid, while for larger values of N the trend of ρ_S is consistent with a noticeable dependence on the cluster size, similarly to what observed for p -H₂ clusters with $22 \leq N \leq 30$. A local minimum is observed for $N=10$; then, the superfluid fraction grows to a value close to 1 for $N=11$ and remains relatively large at $N=12$.

Large fluctuations observed during lengthy simulations render the determination of the value of ρ_S quite difficult for clusters greater than 11 o -D₂ molecules. Nevertheless, we can conclude from our data that clusters of up to 14 molecules still feature a significant superfluid response, which instead is close to zero for larger clusters. As expected, at higher temperatures ρ_S becomes progressively smaller and many-particle permutation cycles are almost absent.

The behavior shown in Fig. 7, indicative of quantum melting, has not been observed for o -D₂ clusters in the temperature range explored in this work. We expect it to be observable at lower temperatures.

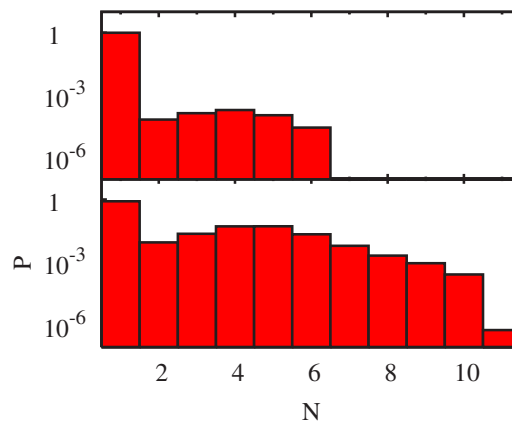


FIG. 13. (Color online) Statistics of permutation cycles involving N molecules for the cluster $(o$ -D₂)₁₁ at $T=0.5$ K (lower panel) and $T=2$ K (upper panel).

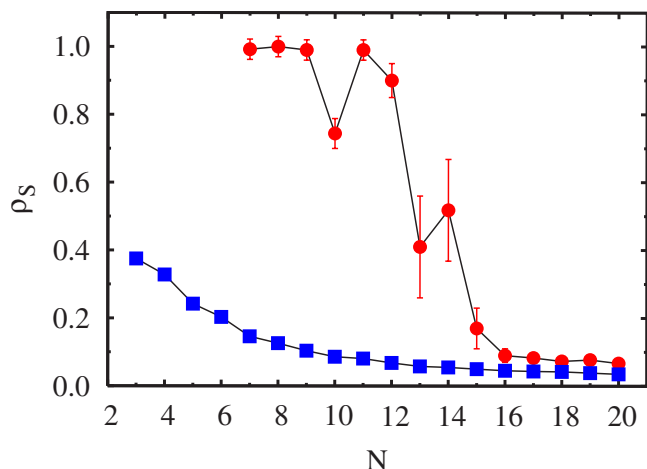


FIG. 14. (Color online) Superfluid fraction of $o\text{-D}_2$ clusters versus cluster size N , at $T=0.5$ K (circles) and $T=2$ K (boxes). When not shown, statistical errors are of the order of, or smaller than, the symbol size. Solid lines are only guides to the eye.

3. Structure

Radial density profiles of the clusters $(o\text{-D}_2)_7$, $(o\text{-D}_2)_{10}$, and $(o\text{-D}_2)_{11}$ at $T=0.5$ K are shown in Fig. 15. The cluster $(o\text{-D}_2)_7$ features a single-shell structure, with a broad peak at about 2.5 \AA , consistent with a high degree of delocalization of the molecules. For $N=10$, the probability of having the center of the system occupied by a molecule becomes significant and the peak is shifted to higher distances by roughly 1 \AA . The shallow minimum which appears at $r \approx 2 \text{ \AA}$ suggests that exchanges are frequent and not restricted to molecules in the first shell; i.e., they involve also the molecule in the center of the cluster.

Important structural differences characterize $(o\text{-D}_2)_{11}$; as shown by the small value of the radial density at the minimum and by the increased height of the first peak in Fig. 15, the molecule in the center of the cluster is strongly localized [see also the high value of $\rho(r \rightarrow 0)$] and scarcely participates

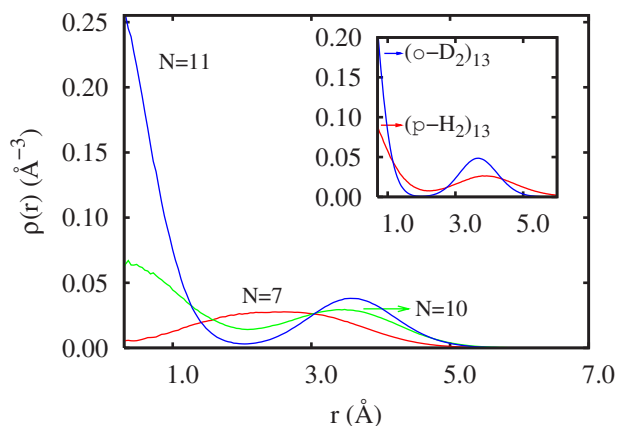


FIG. 15. (Color online) Radial density profiles for $o\text{-D}_2$ clusters with $N=7$, 10 , and 11 , at $T=0.5$ K. The inset shows the radial density profiles of $(o\text{-D}_2)_{13}$ and $(p\text{-H}_2)_{13}$ at the same temperature. Statistical errors, omitted for clarity, are of the order of $5 \times 10^{-4} \text{ \AA}^{-3}$ or less.

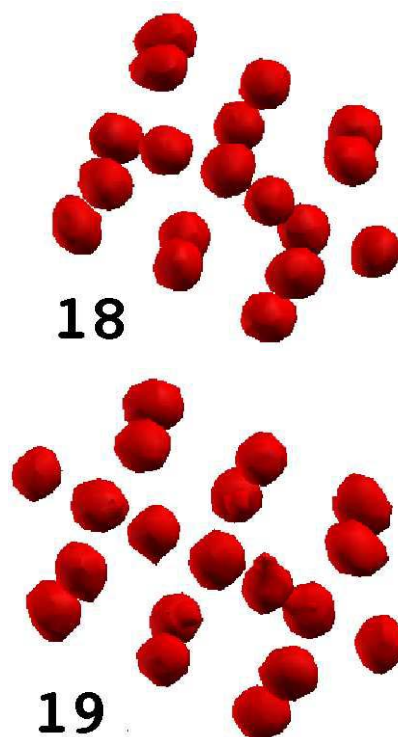


FIG. 16. (Color online) Three-dimensional representation of clusters comprising 18 and 19 $o\text{-D}_2$ molecules, at a temperature of 0.5 K. Both systems have solidlike properties, as molecules enjoy a high degree of localization. However, $(o\text{-D}_2)_{19}$ features greater stability, due to its more symmetric structure (see text).

in multiparticle exchanges. Remarkably, the superfluid fraction of all of these systems is large, close to 1 for $N=7$ and 11 . The inset of Fig. 15 compares radial density profiles of $(o\text{-D}_2)_{13}$ and $(p\text{-H}_2)_{13}$ at $T=0.5$ K; the effect of mass difference on the structural properties is evident. Indeed, the density profile of $(p\text{-H}_2)_{13}$ reflects the liquidlike nature of such a system, whereas in the case of $(o\text{-D}_2)_{13}$, structural details (i.e., pronounced first shell peak and the small value of the radial density at the minimum) are consistent with a more orderly (i.e., solidlike) structure.

It has been already pointed out how local maxima of the chemical potential correspond to magic clusters, featuring greater stability than others (see Fig. 11). Here, we discuss in detail the case of $(o\text{-D}_2)_{19}$. In Fig. 16 we show the three-dimensional structure of clusters comprising $N=18$ and 19 $o\text{-D}_2$ molecules, at $T=0.5$ K. The cluster $(o\text{-D}_2)_{18}$ is made of three rings of five molecules, with the remaining three molecules linearly arranged along the axes of the rings. On adding a single molecule ($N=19$), which also positions itself along the axes of the rings, the structure becomes symmetric with respect to the plane of the central ring. Since both $(o\text{-D}_2)_{18}$ and $(o\text{-D}_2)_{19}$ are solidlike and insulating (i.e., molecules are clearly distinguishable and the value of ρ_s is less than 0.1), the sharp maximum of the chemical potential at $N=19$ appears not to be related to noticeable structural changes (i.e., from more liquidlike to solidlike, as observed for $p\text{-H}_2$ when N increases from 25 to 26), but rather to the pronounced symmetry of this cluster.

IV. CONCLUSIONS

We have studied the low-temperature physical properties of p -H₂ and o -D₂ clusters, of size up to 40 and 20 molecules respectively, using an accurate numerical method. The superfluid fraction of $(p\text{-H}_2)_N$ clusters displays a remarkable dependence on the size N for $22 \leq N \leq 30$, pointing out how the bulk phase emerges nonmonotonically. Coexistence of liquidlike (superfluid) and solidlike (insulating) phases has been shown in some clusters in this size range; the dominance of the first phase at low T indicates that these systems melt as a result of the zero-point motion and quantum exchanges, freezing instead at high T . Superfluid behavior has been also found in o -D₂ clusters of size up to $N=14$. The heavier mass of the o -D₂ molecules is responsible for the suppression of ρ_S in larger clusters. Some clusters, featuring specific numbers of particles, are characterized by greater stability; the fact that the “magic number” $N=13$ is present for both p -H₂ and o -D₂ clusters suggests that its stability is associated with high symmetry; i.e., it is related to the potential energy.

These structures, however, need not necessarily be solidlike, but rather simply have filled coordination shells. Given the intense level of experimental activity in this field, it is to be hoped that some of the predictions made in this work will be soon tested experimentally.

Note added in proof. Recently, we became aware of a manuscript by Khairallah *et al.* [48], also investigating superfluid and structural properties of para-hydrogen clusters by path integral Monte Carlo simulations. Although some of the model interactions utilized therein are not the same as in this work, and therefore a direct comparison is problematic, their results appear in qualitative agreement with ours.

ACKNOWLEDGMENTS

This work was supported by the Natural Science and Engineering Research Council of Canada under research Grant No. 121210893. Simulations were performed on the Mammoth cluster at University of Sherbrooke (Québec, Canada).

-
- [1] V. L. Ginzburg and A. A. Sobyanin, JETP Lett. **15**, 242 (1972).
- [2] Although the fascinating suggestion that a *crystal* may flow without dissipation has been the subject of much recent interest, it is commonly accepted that SF is more easily observed in liquids.
- [3] M. Wagner and D. M. Ceperley, J. Low Temp. Phys. **102**, 275 (1996).
- [4] K. Nho and E. Manousakis, Phys. Rev. B **65**, 115409 (2002).
- [5] M. Boninsegni, Phys. Rev. B **70**, 125405 (2004).
- [6] M. Boninsegni, Phys. Rev. B **70**, 193411 (2004).
- [7] M. C. Gordillo and D. M. Ceperley, Phys. Rev. Lett. **79**, 3010 (1997).
- [8] M. Boninsegni, New J. Phys. **7**, 78 (2005).
- [9] Strictly speaking, of course, “liquid,” “solid,” etc., are only meaningful definitions for bulk phases. In this paper, as is customary in the literature when speaking of clusters, they are used somewhat loosely, with reference to the presence of order, reminiscent of that of a crystal, on a scale comparable to the size of the cluster.
- [10] S. Goyal, D. L. Schutt, and G. Scoles, Phys. Rev. Lett. **69**, 933 (1992).
- [11] S. Grebenev, J. P. Toennies, and A. F. Vilesov, Science **279**, 2083 (1998).
- [12] S. Grebenev, B. Sartakov, J. P. Toennies, and A. F. Vilesov, Science **289**, 1532 (2000).
- [13] E. W. Draeger and D. M. Ceperley, Phys. Rev. Lett. **90**, 065301 (2003).
- [14] S. Moroni, A. Sarsa, S. Fantoni, K. E. Schmidt, and S. Baroni, Phys. Rev. Lett. **90**, 143401 (2003).
- [15] J. Tang, A. R. W. McKellar, F. Mezzacapo, and S. Moroni, Phys. Rev. Lett. **92**, 145503 (2004); F. Mezzacapo, J. Low Temp. Phys. **140**, 241 (2005).
- [16] S. Moroni, N. Blinov, and P. N. Roy, J. Chem. Phys. **121**, 3577 (2004).
- [17] Y. Kwon and K. B. Whaley, Phys. Rev. Lett. **89**, 273401 (2002).
- [18] F. Paesani, R. E. Zillich, Y. Kwon, and K. B. Whaley, J. Chem. Phys. **122**, 181106 (2005).
- [19] Y. Kwon and K. B. Whaley, J. Low Temp. Phys. **140**, 227 (2005).
- [20] S. Baroni and S. Moroni, ChemPhysChem **6**, 1884 (2005).
- [21] S. Moroni, M. Botti, S. de Palo, and A. R. McKellar, J. Chem. Phys. **122**, 094314 (2005).
- [22] P. Sindzingre, D. M. Ceperley, and M. L. Klein, Phys. Rev. Lett. **67**, 1871 (1991).
- [23] F. Mezzacapo and M. Boninsegni, Phys. Rev. Lett. **97**, 045301 (2006).
- [24] M. Boninsegni, Nikolay Prokof'ev, and B. V. Svistunov, Phys. Rev. Lett. **96**, 070601 (2006); Phys. Rev. E **74**, 036701 (2006).
- [25] G. Tejeda, J. M. Fernandez, S. Montero, D. Blume, and J. P. Toennies, Phys. Rev. Lett. **92**, 223401 (2004).
- [26] I. F. Silvera and V. V. Goldman, J. Chem. Phys. **69**, 4209 (1978).
- [27] U. Buck, F. Huisken, A. Kohlhasse, D. Otten, and J. Schaeffer, J. Chem. Phys. **78**, 4439 (1983).
- [28] M. J. Norman, R. O. Watts, and U. Buck, J. Chem. Phys. **81**, 3500 (1984).
- [29] For a discussion of the relative merits of the two potentials, see, for instance, E. Cheng and K. B. Whaley, J. Chem. Phys. **104**, 3155 (1996).
- [30] For a thorough description, see S. Jiang, S. Jiang, and G. A. Voth, J. Chem. Phys. **115**, 7832 (2001).
- [31] The size of the simulation cell turns out to be at least twice the size of the largest cluster considered in this work, which renders PBC's (used for convenience only) immaterial.
- [32] P. Sindzingre, M. L. Klein, and D. M. Ceperley, Phys. Rev. Lett. **63**, 1601 (1989).
- [33] O. Kornilov, J. Navarro, and J. P. Toennies, J. Chem. Phys. **124**, 084307 (2006).
- [34] R. Guardiola and J. Navarro, Phys. Rev. A **74**, 025201 (2006).

- [35] We have computed energetics of several clusters at T lower than 1 K and estimate the maximum difference between our results at $T=1$ K and those extrapolated to $T=0$ to be less than 0.3 K.
- [36] J. E. Cuervo and P. N. Roy, *J. Chem. Phys.* **125**, 124314 (2006).
- [37] D. Blume (unpublished).
- [38] The results presented here are consistent with those reported in Ref. [23], once statistical uncertainties are properly taken into account. The estimates of ρ_S presented in this work benefit from much longer computer runs than those of Ref. [23], hence their smaller statistical uncertainties.
- [39] D. Scharf, M. L. Klein, and G. J. Martyna, *J. Chem. Phys.* **97**, 3590 (1992).
- [40] See, for instance, G. G. Batrouni and R. T. Scalettar, *Phys. Rev. Lett.* **84**, 1599 (2000).
- [41] We define a *sweep* as a sampling cycle which starts with the opening and ends with the closing of a worm (for details, see Ref. [24]).
- [42] R. E. Kunz and R. S. Berry, *Phys. Rev. Lett.* **71**, 3987 (1993).
- [43] C. Predescu, P. A. Frantsuzov, and V. A. Mandelshtam, *J. Chem. Phys.* **122**, 154305 (2005).
- [44] F. Calvo, J. P. K. Doye, and D. J. Wales, *J. Chem. Phys.* **114**, 7312 (2001).
- [45] C. Predescu, D. Sabo, and J. D. Doll, *J. Chem. Phys.* **119**, 12119 (2001).
- [46] P. A. Frantsuzov, D. Meluzzi, and V. A. Mandelshtam, *Phys. Rev. Lett.* **96**, 113401 (2006).
- [47] Molecular *ortho*-deuterium naturally occurs as a mixture of $S=0$ and $S=2$ spin states.
- [48] S. A. Khairallah, M. B. Sevryuk, D. M. Ceperley, and J. P. Toennies, e-print physics/0612161.